Performance Analysis of Space–Time Block Codes Over Keyhole Nakagami-m Fading Channels

Hyundong Shin, *Student Member, IEEE,* and Jae Hong Lee, *Senior Member, IEEE*

***Abstract*—In multiple-input–multiple-output (MIMO) fading environments, degenerate channel phenomena, called *keyholes* or *pinholes*, may exist under the realistic assumption that the spatial fading is uncorrelated at the transmitter and the receiver, but the channel has a rank-deficient transfer matrix. In this paper, we analyze the exact average symbol error rate (SER) of orthogonal space–time block codes (STBCs) with M-PSK and M-QAM constellations over Nakagami-m fading channels in the presence of the keyhole. We derive the moment generating function (MGF) of instantaneous signal-to-noise ratio (SNR) after space–time block decoding (signal combining) in such channels. Using a well-known MGF-based analysis approach, we express the average SER of the STBC in the form of single finite-range integrals whose integrand contains only the derived MGF. Numerical results show that the keyhole significantly degrades the SER performance of the STBC from idealistic behaviors in independent identically distributed MIMO channels.**

***Index Terms*—Diversity, keyhole, multiple-input–multiple-output (MIMO) channels, Nakagami fading, space–time block codes, symbol error rate (SER).**

I. Introduction

In research areas on wireless communications, multiple-input–multiple-output (MIMO) systems equipped with the multielement antenna arrays at both transmit and receive ends have recently drawn considerable attention in response to the increasing requirements on high data rate and reliability in radio links. More recently, in MIMO fading environments, the existence of rank-deficient (*keyhole* or *pinhole*) channels has been proposed and demonstrated through physical examples that have uncorrelated spatial fading, but only have a single or reduced degree of freedom [1]–[4]. This rank deficiency reduces achievable spectral efficiency and link quality in MIMO systems.

One of the most promising approaches to use MIMO channels is signal processing and modulation techniques to maximize the diversity gain [5]–[8]. Space–time block coding is a modulation scheme for the use of multiple transmit antennas providing a simple transmit diversity scheme with the same diversity order as maximal-ratio receiver combining [7]–[9]. Due to the orthogonal structure of space–time block codes (STBCs), maximum likelihood (ML) decoding can be implemented by using the single-symbol decoding based on linear processing at the receiver. It is well known that the orthogonal space–time block encoding and decoding (signal combining) transform a MIMO fading channel into an equivalent single-input–single-output (SISO) Gaussian channel with a path gain of the squared Frobenius (or Hilbert–Schmidt) norm of the channel matrix [10]–[13]. In [14], it is also shown that the orthogonal STBCs are optimal in terms of the signal-to-noise ratio (SNR).

In this paper, we study the effect of keyholes on the symbol error rate (SER) of the orthogonal STBC with the assumption that the rich multiple scattering at the transmit and receive arrays may result in independent Nakagami-m fading. In this case, the fading between each pair of the transmit and receive antennas in the presence of the keyhole is characterized by *double Nakagami-m fading*, i.e., a product of two independent Nakagami-m distributions. This is a generalization of the statistical model used in [1] and [2], where the fading is characterized by *double Rayleigh fading*—that is, each entry of the channel matrix was assumed to be a product of two independent zero-mean complex Gaussian random variables, in contrast to the complex Gaussian that is normally assumed in wireless channels—for keyhole channels. In order to evaluate the exact average SER of the orthogonal STBC with M-ary phase-shift keying (M-PSK) and M-ary quadrature amplitude modulation (M-QAM) constellations over keyhole Nakagami-m fading channels, we first derive the moment generating function (MGF) of instantaneous SNR after space–time block decoding in this propagation scenario. We then use the MGF-based approach for evaluating the error performance over fading channels developed by using alternative representations of the Gaussian and Marcum Q-functions [16]–[19]. This MGF-based approach does not attempt to compute the probability density function (pdf) of instantaneous SNR. Once the MGF is available, the average SER can be expressed in terms of a finite-range integral involving only the derived MGF. In addition, we obtain an expression for the average SER of the STBC over normal independent and identically distributed (i.i.d.) Nakagami-m fading channels (i.e., i.i.d. Nakagami-m MIMO channels without the keyhole phenomenon) in terms of higher transcendental functions, such as the Gauss and Appell hypergeometric functions [24]. These expressions hold for *arbitrary* real-valued fading index $m \geq 0.5$. To the authors' best knowledge, no closed-form solutions to the average SER of M-ary signals over Nakagami-m fading channels with single and multichannel reception are available for arbitrary m. Previous closed-form solutions are restricted to integer values of m or noncoherent detection of orthogonal M-ary frequency-shift keying (M-FSK) (e.g., see [17]–[19] and the references therein).

Manuscript received August 10, 2002; revised June 2, 2003 and September 22, 2003. This work was supported in part by the National Research Laboratory (NRL) Program and the Brain Korea 21 Project.

The authors are with the School of Electrical Engineering, Seoul National University, Seoul 151-742, Korea (e-mail: shd71@snu.ac.kr).

Digital Object Identifier 10.1109/TVT.2004.823540

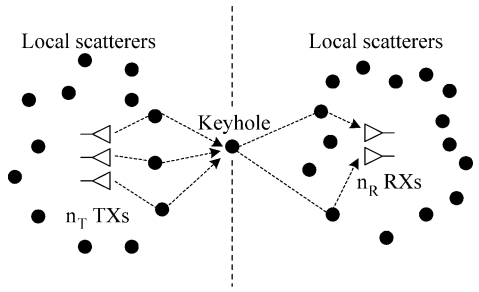

Fig. 1. Keyhole MIMO channels.

The i.i.d. and single keyhole channels considered in this paper are two extreme cases of spatially uncorrelated MIMO channels [20].

The remainder of this paper is organized as follows. The next section presents the channel model that is under consideration and brief overview of the STBC. In Section III, we derive the MGF of instantaneous SNR after space–time block decoding. Section IV gives the average SER of the orthogonal STBC with M-PSK and M-QAM constellations over i.i.d./keyhole Nakagami-m fading channels. Simulation and numerical results are also presented in Section V. Finally, the main points are summarized in Section VI.

II. System Model

We consider a MIMO wireless communication system with n_T transmit and n_R receive antennas.

A. Keyhole and Channel Models

Assuming a nonline of sight, local scattering model at both transmit and receive sides for outdoor transmission, scatterers are placed randomly close to either the transmit or receive array. Furthermore, the arrangement of scatterers is assumed to be quasistatic; therefore, the random arrangement will change at certain intervals. In general, this leads to a quasistatic, frequency-flat, and uncorrelated MIMO channel for narrow-band signals. However, in certain environments the channel degeneracy may arise due to the keyhole or pinhole effect (for details, see [2] and [3]), as shown in Fig. 1. The only way for the radio wave to propagate from the transmitter to the receiver is to pass through the keyhole. In this case, the channel matrix $\mathbf{H}$ for MIMO channels is given by (1), shown at the bottom of the page. In (1), $\{\alpha_j e^{\boldsymbol{j}\varphi_j}\}_{j=1}^{n_T}$ and $\{\beta_i e^{\boldsymbol{j}\vartheta_i}\}_{i=1}^{n_R}$ describe the rich scattering at the transmit and receive arrays, respectively, and $\boldsymbol{j}=\sqrt{-1}$. The (i,j)th entry h_{ij} of $\mathbf{H}$ represents a complex channel coefficient from the jth transmit antenna to the ith receive antenna. For a more general model, we assume that $\{\alpha_j\}_{j=1}^{n_T}$ and $\{\beta_i\}_{i=1}^{n_R}$ are i.i.d. Nakagami-m variates with fading severity parameters m_T and m_R, respectively, namely

$$p_{\alpha_j}(\alpha)=\frac{2}{\Gamma(m_T)}\left(\frac{m_T}{\Omega_T}\right)^{m_T}\alpha^{2m_T-1}e^{\frac{-m_T\alpha^2}{\Omega_T}},\quad \alpha\geq 0,\ m_T\geq 0.5,\ j=1,2,\ldots,n_T \tag{2}$$

$$p_{\beta_i}(\beta)=\frac{2}{\Gamma(m_R)}\left(\frac{m_R}{\Omega_R}\right)^{m_R}\beta^{2m_R-1}e^{\frac{-m_R\beta^2}{\Omega_R}},\quad \beta\geq 0,\ m_R\geq 0.5,\ i=1,2,\ldots,n_R \tag{3}$$

where $\Omega_T=E[\alpha_i^2]$, $\Omega_R=E[\beta_j^2]$, and $\Gamma(\cdot)$ is the gamma function. All of the channel phase shifts $\{\varphi_j\}_{j=1}^{n_T}$ and $\{\vartheta_i\}_{i=1}^{n_R}$ are assumed to be independent and uniformly distributed over $[0,2\pi)$. Furthermore, we assume that the keyhole ideally reradiates the captured energy, like the transmit and receive scatterers, and that each entry of $\mathbf{H}$ has a unit power, i.e., $E[|h_{ij}|^2]=\Omega_T\cdot\Omega_R=1$ for all $i=1,2,\ldots,n_R$ and $j=1,2,\ldots,n_T$. Note that as all of $\alpha_j e^{\boldsymbol{j}\varphi_j}$ and $\beta_i e^{\boldsymbol{j}\vartheta_i}$ are independent, all entries of the channel matrix $\mathbf{H}$ are uncorrelated, but rank $(\mathbf{H})=1$.

B. Space–Time Block Codes

Fig. 2 shows a space–time block-coded MIMO system. Nb information bits are mapped as symbols $s_1,s_2,\ldots,s_N$, which are selected from the M-PSK or M-QAM signal constellation $\mathcal{A}$ with average energy E_0 by Gray mapping, where $b=\log_2 M$. Then, $\{s_n\}_{n=1}^{N}$ are encoded by a space–time block code defined by a $p\times n_T$ column orthogonal transmission matrix $\mathcal{G}$

$$\mathcal{G}=\begin{pmatrix} g_{11} & g_{12} & \cdots & g_{1n_T}\\ g_{21} & g_{22} & \cdots & g_{2n_T}\\ \vdots & \vdots & \ddots & \vdots\\ g_{p1} & g_{p2} & \cdots & g_{pn_T}\end{pmatrix} \tag{4}$$

where the entries g_{kj}, $k=1,2,\ldots,p$, and $j=1,2,\ldots,n_T$ are linear combinations of $s_1,s_2,\ldots,s_N$ and their conjugates [8], [9]. At each time slot k, signals $\{g_{kj}\}_{j=1}^{n_T}$ are transmitted simultaneously through n_T transmit antennas. Since p symbol durations are necessary to transmit N symbols, the rate R of the STBC is $R=N/p$. For instance, the STBC $\mathcal{G}_2$, first proposed

$$\mathbf{H}=\begin{pmatrix}\beta_1 e^{\boldsymbol{j}\vartheta_1}\\ \beta_2 e^{\boldsymbol{j}\vartheta_2}\\ \vdots\\ \beta_{n_R}e^{\boldsymbol{j}\vartheta_{n_R}}\end{pmatrix}\begin{pmatrix}\alpha_1 e^{\boldsymbol{j}\varphi_1} & \alpha_2 e^{\boldsymbol{j}\varphi_2} & \cdots & \alpha_{n_T}e^{\boldsymbol{j}\varphi_{n_T}}\end{pmatrix}$$
$$=\begin{pmatrix}\alpha_1\beta_1 e^{\boldsymbol{j}(\varphi_1+\vartheta_1)} & \alpha_2\beta_1 e^{\boldsymbol{j}(\varphi_2+\vartheta_1)} & \cdots & \alpha_{n_T}\beta_1 e^{\boldsymbol{j}(\varphi_{n_T}+\vartheta_1)}\\ \alpha_1\beta_2 e^{\boldsymbol{j}(\varphi_1+\vartheta_2)} & \alpha_2\beta_2 e^{\boldsymbol{j}(\varphi_2+\vartheta_2)} & \cdots & \alpha_{n_T}\beta_2 e^{\boldsymbol{j}(\varphi_{n_T}+\vartheta_2)}\\ \vdots & \vdots & \ddots & \vdots\\ \alpha_1\beta_{n_R}e^{\boldsymbol{j}(\varphi_1+\vartheta_{n_R})} & \alpha_2\beta_{n_R}e^{\boldsymbol{j}(\varphi_2+\vartheta_{n_R})} & \cdots & \alpha_{n_T}\beta_{n_R}e^{\boldsymbol{j}(\varphi_{n_T}+\vartheta_{n_R})}\end{pmatrix}. \tag{1}$$

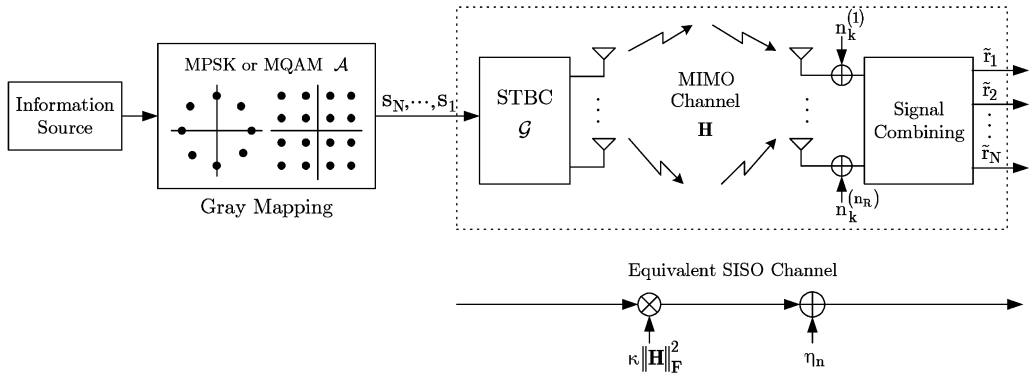

Fig. 2. Space–time block-coded MIMO system and its equivalent SISO model.

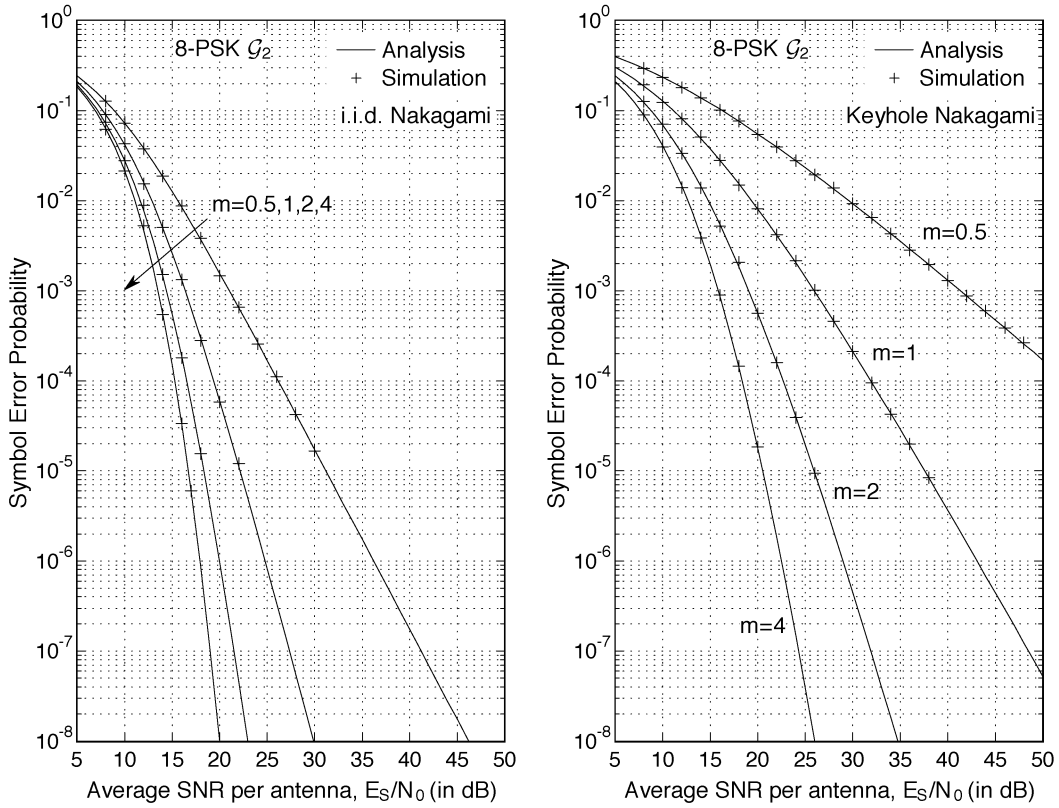

Fig. 3. SER versus average SNR per receive antenna for the STBC $\mathcal{G}_2$ with 8-PSK over i.i.d. and keyhole Nakagami-m fading channels. $n_R = 2$ and $m_T = m_R = m$ for keyhole channels.

by Alamouti in [7], is a one-rate code employing two transmit antennas, defined by

$$\mathcal{G} = \begin{pmatrix} s_1 & s_2 \\ -s_2^* & s_1^* \end{pmatrix} \tag{5}$$

where $*$ represents the complex conjugate.

At the receiver, the signal received by the ith antenna in the kth time slot is given by

$$r_k^{(i)} = \sum_{j=1}^{n_T} h_{ij} g_{kj} + n_k^{(i)} \tag{6}$$

where $n_k^{(i)}$ is a zero-mean complex Gaussian noise with variance $N_0/2$ per dimension. The average energy of the symbols transmitted from each antenna is assumed to be E_s/n_T so that the average power of the received signal at each receive antenna is equal to $(E_s/n_T)\sum_{j=1}^{n_T} E[|h_{ij}|^2] = E_s$ and the SNR per receive antenna is E_s/N_0. With perfect channel-state information, the ML receiver computes the decision metric [9]

$$D = \sum_{k=1}^{p} \sum_{i=1}^{n_R} \left| r_k^{(i)} - \sum_{j=1}^{n_T} h_{ij} g_{kj} \right|^2 \tag{7}$$

over all codewords and decides in favor of the codeword that minimizes the sum D.

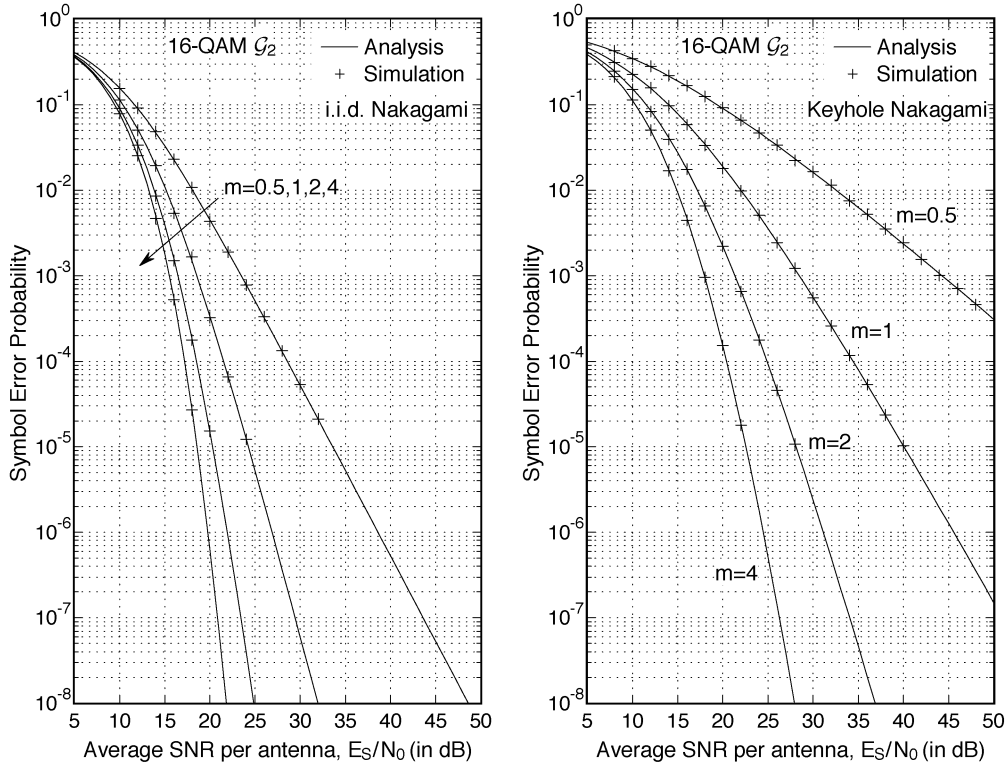

Fig. 4. SER versus average SNR per receive antenna for the STBC $\mathcal{G}_2$ with 16-QAM over i.i.d. and keyhole Nakagami-m fading channels. $n_R = 2$ and $m_T = m_R = m$ for keyhole channels.

Let E_{tot} be the total average energy of a block, i.e., $E_{\text{tot}} = E[\|\mathcal{G}\|_F^2] = p \cdot E_s$ where $\|\mathcal{G}\|^2$ is the squared Frobenius norm[1] of the matrix $\mathcal{G}$. From the column orthogonal property of the matrix $\mathcal{G}$ [8], E_{tot} can be also written as

$$\begin{aligned} E_{\text{tot}} &= E\left[\text{tr}(\mathcal{G}\mathcal{G}^\dagger)\right] \\ &= E\left[\text{tr}\left\{\left(\kappa \cdot \sum_{n=1}^{N} |s_n|^2\right)\mathbf{I}\right\}\right] \\ &= n_T \cdot \kappa \cdot N \cdot E_0 \end{aligned} \tag{8}$$

where $\mathbf{I}$ is the $n_T \times n_T$ identity matrix and κ is a constant depending on the matrix $\mathcal{G}$. For example, $\kappa = 1$ for $\mathcal{G}_2$, $\mathcal{H}_3$, and $\mathcal{H}_4$ in [9] and $\kappa = 2$ for $\mathcal{G}_3$ and $\mathcal{G}_4$ in [9]. From (8), we get the average energy of the constellation $\mathcal{A}$ as

$$E_0 = \frac{p \cdot E_s}{n_T \cdot \kappa \cdot N} = \frac{E_s}{n_T \cdot \kappa \cdot R}. \tag{9}$$

III. MGF of Instantaneous SNR After Space–Time Block Decoding

Due to the orthogonality of $\mathcal{G}$'s columns, the metric D in (7) can decompose into N parts, which are only a function of $s_n, n = 1, 2, \ldots, N$, respectively [9], [10]. Consequently, the minimization of (7) is equivalent to minimizing each decision metric for s_n separately and the ML receiver chooses $\hat{s}_n$ for $s_n, n = 1, 2, \cdots, N$, if and only if [10]

$$\hat{s}_n = \arg\min_{s \in \mathcal{A}} \left| \underbrace{\left(\kappa \|\mathbf{H}\|_F^2 s_n + \eta_n\right)}_{\triangleq \tilde{r}_n} - \kappa \|\mathbf{H}\|_F^2 s \right|^2 \tag{10}$$

where $\tilde{r}_n$ and $\eta_n \sim \mathcal{CN}(0, \kappa\|\mathbf{H}\|_F^2 N_0)$ are the combiner output and Gaussian noise for after space–time block decoding, respectively.[2] From (10), we see that orthogonal space–time block encoding and decoding (signal combining) transform a MIMO fading channel into an equivalent SISO channel. The price of this simple decoding structure for the orthogonal STBC is the loss in the data rate, because the rate of orthogonal STBCs over arbitrary complex constellations is less than the full rate if the number of transmit antennas is greater than two. From (9) and (10), we have the instantaneous SNR per symbol after space–time block decoding as

$$\gamma_{\text{STBC}} = \frac{\kappa^2 \|\mathbf{H}\|_F^4 E_0}{\kappa \|\mathbf{H}\|_F^2 N_0} = \frac{\|\mathbf{H}\|_F^2 E_s}{n_T R N_0} \tag{11}$$

which states that the performance of STBCs depends on the statistical property of the squared Frobenius norm of the channel matrix.

[1]The squared Frobenius norm of a $p \times q$ matrix $\mathbf{A}$ is defined as

$$\|\mathbf{A}\|_F^2 \triangleq \text{tr}(\mathbf{A}\mathbf{A}^\dagger) = \sum_{i=1}^{p}\sum_{j=1}^{q} |a_{ij}|^2$$

where $\text{tr}(\cdot)$ and $\dagger$ denote the trace operator and the transpose conjugate of a matrix, respectively.

[2]See (17) and (20) in [10], where the constant κ was assumed to be 1.

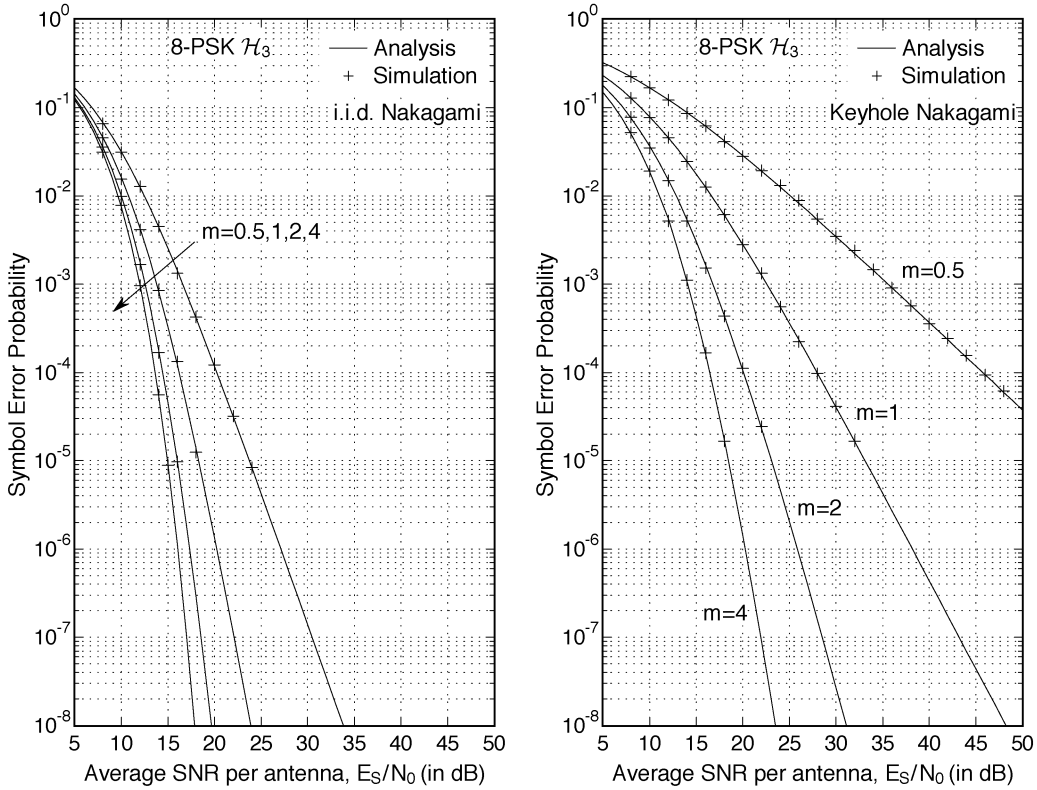

Fig. 5. SER versus average SNR per receive antenna for the STBC $\mathcal{H}_3$ with 8–PSK over i.i.d. and keyhole Nakagami-m fading channels. $n_R = 2$ and $m_T = m_R = m$ for keyhole channels.

A. MGF of γ_{STBC}

In the following, we derive the MGF of γ_{STBC}, which is used to evaluate the SER of the STBC in the next section. To this end, we first derive the MGF of $\|\mathbf{H}\|_F^2$.

Let $U = \sum_{j=1}^{n_T} \alpha_j^2$ and $V = \sum_{i=1}^{n_R} \beta_i^2$. Then we can rewrite the squared Frobenius norm of the channel matrix as

$$\|\mathbf{H}\|_F^2 = \sum_{i=1}^{n_R}\sum_{j=1}^{n_T} \alpha_j^2 \cdot \beta_i^2 = \sum_{j=1}^{n_T} \alpha_j^2 \cdot \sum_{i=1}^{n_R} \beta_i^2 = U \cdot V. \quad (12)$$

Since α_j and β_i are Nakagami-m distributed, α_j^2 and β_i^2 follow the gamma distribution, i.e., $\alpha_j^2 \sim \Upsilon(\Omega_T/m_T, m_T)$ and $\beta_i^2 \sim \Upsilon(\Omega_R/m_R, m_R)$ [17].[3] Moreover, the sum of n statistically independent gamma variates with shape parameters c_i, $i = 1, 2, \ldots, n$, and a common scale parameter b is also a gamma variate with the shape parameter $\sum_{i=1}^{n} c_i$ and scale parameter b [22]. Therefore, U and V are gamma distributed, i.e., $U \sim \Upsilon(\Omega_T/m_T, m_T n_T)$ and $V \sim \Upsilon(\Omega_R/m_R, m_R n_R)$. According to the result of (34) in Appendix A, we can obtain the MGF of $\|\mathbf{H}\|_F^2$ as

$$\phi_{\|\mathbf{H}\|_F^2}(s) = {}_2F_0\left(m_T n_T, m_R n_R; ; -\frac{s}{m_T m_R}\right). \quad (13)$$

[3]We use the shorthand notation $X \sim \Upsilon(b, c)$ to denote that X is gamma distributed with a *scale parameter* $b > 0$ and a *shape parameter* $c > 0$, namely [22, ch. 19]

$$p_X(x) = \frac{x^{c-1}}{\Gamma(c) b^c} e^{-\frac{x}{b}}, \quad x \geq 0.$$

If $n_T = n_R = 1$ and $m_T = m_R = 1$ (i.e., *double Rayleigh-fading* channels), then the MGF (13) reduce to

$$\phi_{\|\mathbf{H}\|_F^2}(s) = \frac{e^{\frac{1}{s}}}{s}\Gamma\left(0, \frac{1}{s}\right) \quad (14)$$

where $\Gamma(n, z) \triangleq \int_z^\infty e^{-t} t^{n-1} dt$ is the complementary incomplete gamma function [23, (8.350.2)].

From (11) and (13), the MGF of γ_{STBC} for keyhole MIMO channels can be readily written as

$$\begin{aligned}\phi_{\gamma_{\mathrm{STBC}}}^{\mathrm{keyhole}}(s) &\triangleq \int_0^\infty e^{-s\gamma} \cdot p_{\gamma_{\mathrm{STBC}}}^{\mathrm{keyhole}}(\gamma) d\gamma \\ &= \phi_{\|\mathbf{H}\|_F^2}\left(s \cdot \frac{\frac{E_s}{N_0}}{n_T R}\right) \\ &= {}_2F_0\left(m_T n_T, m_R n_R; ; -\frac{\frac{sE_s}{N_0}}{m_T m_R n_T R}\right) \quad (15)\end{aligned}$$

where $p_{\gamma_{\mathrm{STBC}}}^{\mathrm{keyhole}}(\gamma)$ is the probability density function (pdf) of instantaneous SNR after space–time block decoding for keyhole Nakagami-m fading channels. Note that, for normal i.i.d. Nakagami-m MIMO channels in the absence of the keyhole, $\|\mathbf{H}\|_F^2$ is the sum of $n_T n_R$ i.i.d. gamma variates and then the MGF of γ_{STBC} can be easily written as

$$\begin{aligned}\phi_{\gamma_{\mathrm{STBC}}}^{\mathrm{i.i.d.}}(s) &\triangleq \int_0^\infty e^{-s\gamma} \cdot p_{\gamma_{\mathrm{STBC}}}^{\mathrm{i.i.d.}}(\gamma) d\gamma \\ &= \left(1 + \frac{\frac{sE_s}{N_0}}{m n_T R}\right)^{-m n_T n_R} \quad (16)\end{aligned}$$

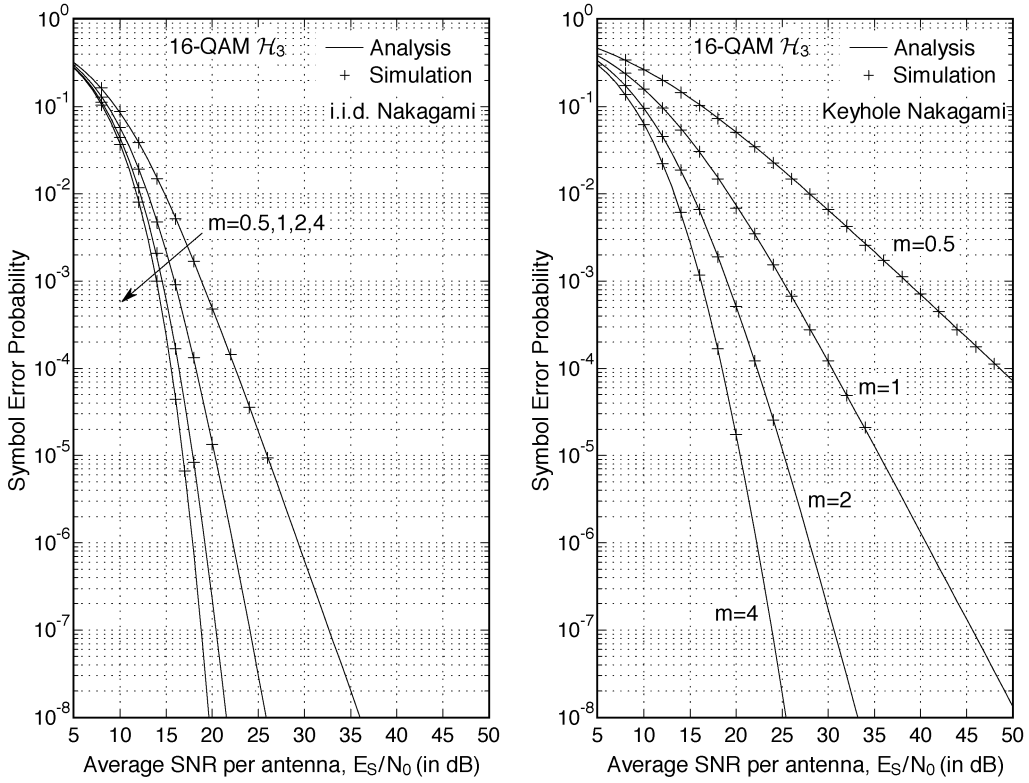

Fig. 6. SER versus average SNR per receive antenna for the STBC $\mathcal{H}_3$ with 16-QAM over i.i.d. and keyhole Nakagami-m fading channels. $n_R = 2$ and $m_T = m_R = m$ for keyhole channels.

where $p^{\text{i.i.d.}}_{\gamma_{\text{STBC}}}(\gamma)$ is the pdf of instantaneous SNR after space–time block decoding for i.i.d. Nakagami-m fading channels.

B. Amount of Fading

The amount of fading (AF) is a unified measure of the severity of the fading defined by the ratio of the variance of the received energy to the square of the average received energy [17, ch. 2], [21]. For a space–time block-coded MIMO link, we have

$$\text{AF}_{\text{STBC}} \triangleq \frac{\text{Var}[\gamma_{\text{STBC}}]}{\left(E[\gamma_{\text{STBC}}]\right)^2} = \frac{E\left[\|\mathbf{H}\|_F^4\right] - \left(E\left[\|\mathbf{H}\|_F^2\right]\right)^2}{\left(E\left[\|\mathbf{H}\|_F^2\right]\right)^2}. \tag{17}$$

Let us now consider a keyhole channel with $m_T = m_R = m$. From (11), (12), and (35), we obtain the AF for the space–time block-coded keyhole MIMO channel in the form

$$\text{AF}^{\text{keyhole}}_{\text{STBC}} = \frac{n_T + n_R + \frac{1}{m}}{m n_T n_R} \tag{18}$$

which reveals that the severity of the fading is increased by a factor of $(n_T + n_R + 1/m)$ due to the keyhole, as compared to $\text{AF}^{\text{iid}}_{\text{STBC}} = 1/(m n_T n_R)$ for the i.i.d. case. The case that $\text{AF}^{\text{keyhole}}_{\text{STBC}} > 1$ corresponds to fading situations more severe than Rayleigh fading without diversity.

IV. AVERAGE SER

From the MGF of γ_{STBC} in previous section, we can evaluate the SER of the orthogonal STBC over i.i.d. and keyhole Nakagami-m fading channels by using a well-known MGF-based approach for evaluating the error performance of a digital communication system over fading channels [16], [17].

A. i.i.d. Nakagami-m Fading Channels

The conditional SER for coherent M-PSK signals is given by [16], [17]

$$P_s^{\text{MPSK}}(E|\gamma) = \frac{1}{\pi}\int_0^{\pi-\frac{\pi}{M}} \exp\left(-\frac{\gamma g_{\text{MPSK}}}{\sin^2\theta}\right) d\theta \tag{19}$$

where $g_{\text{MPSK}} = \sin^2(\pi/M)$. Averaging (19) over the pdf $p^{\text{i.i.d.}}_{\gamma_{\text{STBC}}}(\gamma)$ and using (16), the average SER of the STBC with M-PSK modulation over i.i.d. Nakagami-m fading channels is given by

$$P^{\text{MPSK}}_{s,\text{i.i.d.}}(E) = \frac{1}{\pi}\int_0^{\infty}\int_0^{\pi-\frac{\pi}{M}} \exp\left(-\frac{\gamma g_{\text{MPSK}}}{\sin^2\theta}\right) p^{\text{i.i.d.}}_{\gamma_{\text{STBC}}}(\gamma) d\theta d\gamma = \frac{1}{\pi}\int_0^{\pi-\frac{\pi}{M}} \phi^{\text{i.i.d.}}_{\gamma_{\text{STBC}}}\left(\frac{g_{\text{MPSK}}}{\sin^2\theta}\right) d\theta. \tag{20}$$

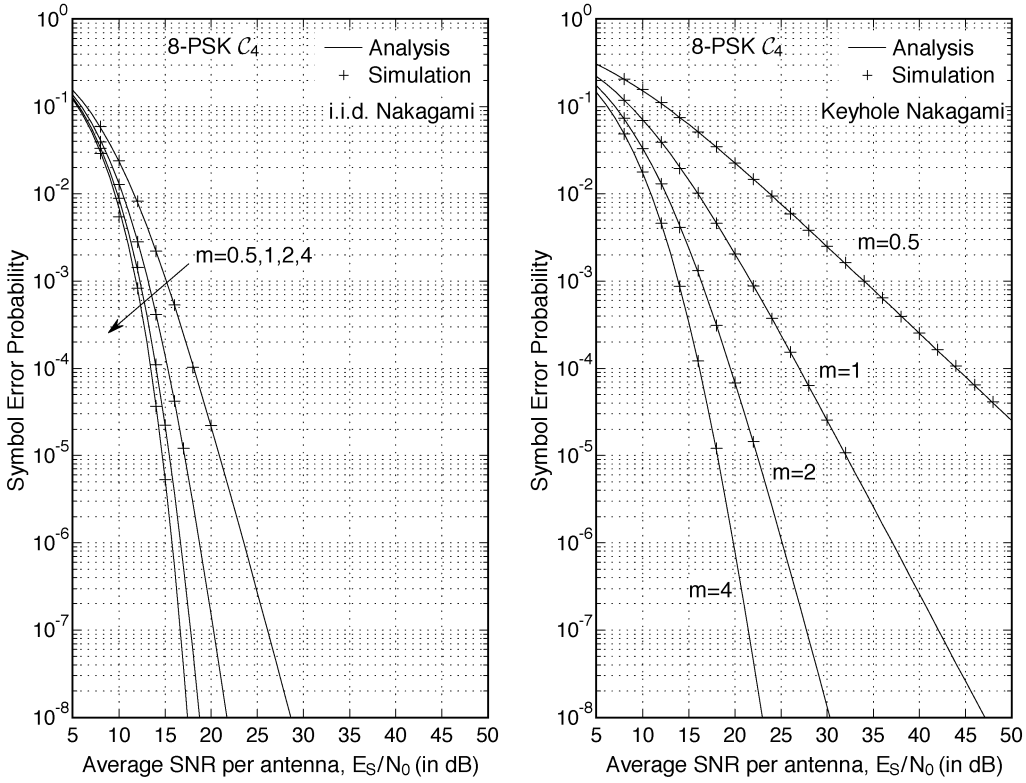

Fig. 7. Symbol error rates versus average SNR per receive antenna for the STBC $\mathcal{C}_4$ with 8-PSK over i.i.d. and keyhole Nakagami-m fading channels. $n_R = 2$; $m_T = m_R = m$ for keyhole channels.

The conditional SER for coherent square M-QAM signals is given by [16], [17]

$$P_s^{\mathrm{MQAM}}(E|\gamma) = \frac{4q}{\pi}\int_0^{\frac{\pi}{2}} \exp\left(-\frac{\gamma g_{\mathrm{MQAM}}}{\sin^2\theta}\right) d\theta - \frac{4q^2}{\pi}\int_0^{\frac{\pi}{4}} \exp\left(-\frac{\gamma g_{\mathrm{MQAM}}}{\sin^2\theta}\right) d\theta \tag{21}$$

where $q = 1-1/\sqrt{M}$ and $g_{\mathrm{MQAM}} = 3/(2(M-1))$. Similar to (20), the average SER of the STBC with M-QAM modulation over i.i.d. Nakagami-m fading channels can be readily shown as

$$P_{s,\mathrm{i.i.d.}}^{\mathrm{MQAM}}(E) = \frac{4q}{\pi}\int_0^{\frac{\pi}{2}} \phi_{\gamma_{\mathrm{STBC}}}^{\mathrm{i.i.d.}}\left(\frac{g_{\mathrm{MQAM}}}{\sin^2\theta}\right) d\theta - \frac{4q^2}{\pi}\int_0^{\frac{\pi}{4}} \phi_{\gamma_{\mathrm{STBC}}}^{\mathrm{i.i.d.}}\left(\frac{g_{\mathrm{MQAM}}}{\sin^2\theta}\right) d\theta. \tag{22}$$

$$\begin{aligned} P_{s,\mathrm{i.i.d.}}^{\mathrm{MPSK}}(E) &= \mathcal{J}_{mn_Tn_R}\left(\frac{\xi_{\mathrm{MPSK}}E_s}{N_0}, \frac{\pi}{M}\right) \\ &= \phi_{\gamma_{\mathrm{STBC}}}^{\mathrm{i.i.d.}}(g_{\mathrm{MPSK}})\left\{\frac{1}{2\sqrt{\pi}}\frac{\Gamma\left(mn_Tn_R+\frac{1}{2}\right)}{\Gamma(mn_Tn_R+1)}{}_2F_1\left(mn_Tn_R, \frac{1}{2}; mn_Tn_R+1; \frac{1}{1+\frac{\xi_{\mathrm{MPSK}}E_s}{N_0}}\right)\right. \\ &\qquad \left. + \frac{\sqrt{1-g_{\mathrm{MPSK}}}}{\pi}F_1\left(\frac{1}{2}, mn_Tn_R, \frac{1}{2}-mn_Tn_R; \frac{3}{2}; \frac{1-g_{\mathrm{MPSK}}}{1+\frac{\xi_{\mathrm{MPSK}}E_s}{N_0}}, 1-g_{\mathrm{MPSK}}\right)\right\}. \end{aligned} \tag{23}$$

$$\begin{aligned} P_{s,\mathrm{i.i.d.}}^{\mathrm{MQAM}}(E) &= 4q\cdot\mathcal{J}_{mn_Tn_R}\left(\frac{\xi_{\mathrm{MQAM}}E_s}{N_0}, \frac{\pi}{2}\right) - 4q^2\cdot\mathcal{F}_{mn_Tn_R}\left(\frac{\xi_{\mathrm{MQAM}}E_s}{N_0}\right) \\ &= \frac{2q\phi_{\gamma_{\mathrm{STBC}}}^{\mathrm{i.i.d.}}(g_{\mathrm{MQAM}})}{\sqrt{\pi}}\frac{\Gamma\left(mn_Tn_R+\frac{1}{2}\right)}{\Gamma(mn_Tn_R+1)}{}_2F_1\left(mn_Tn_R, \frac{1}{2}; mn_Tn_R+1; \frac{1}{1+\frac{\xi_{\mathrm{MQAM}}E_s}{N_0}}\right) \\ &\quad - \frac{2q^2}{\pi}\frac{\phi_{\gamma_{\mathrm{STBC}}}^{\mathrm{i.i.d.}}(2g_{\mathrm{MQAM}})}{2mn_Tn_R+1}F_1\left(1, mn_Tn_R, 1; mn_Tn_R+\frac{3}{2}; \frac{1+\frac{\xi_{\mathrm{MQAM}}E_s}{N_0}}{1+\frac{2\xi_{\mathrm{MQAM}}E_s}{N_0}}, \frac{1}{2}\right). \end{aligned} \tag{24}$$

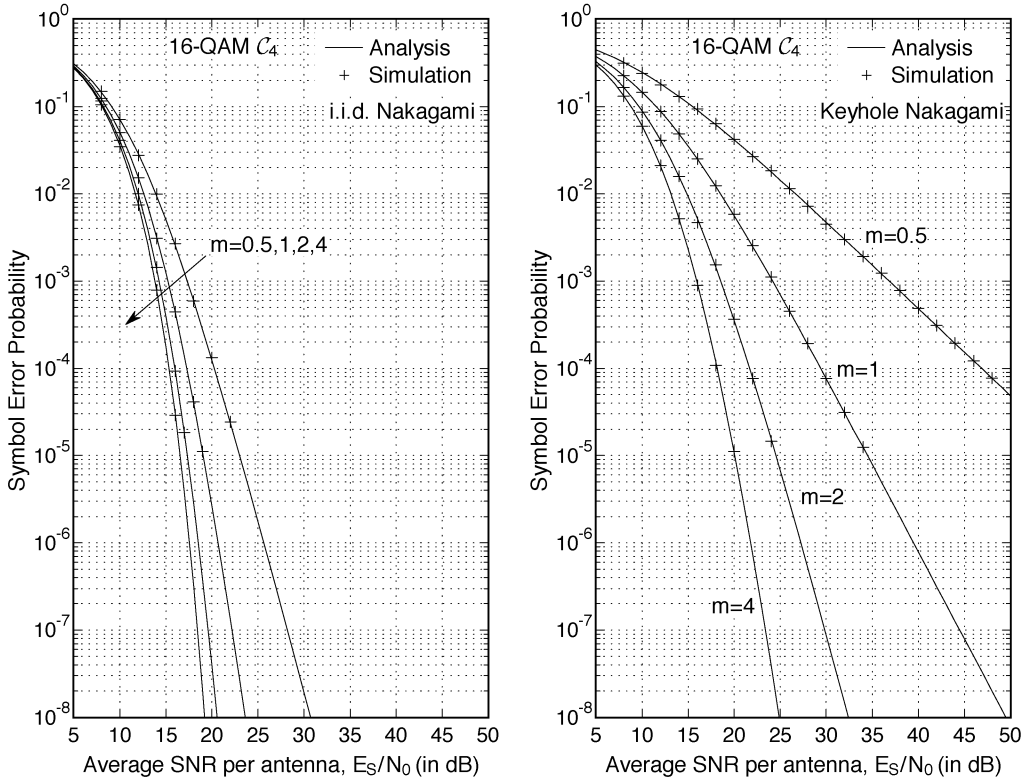

Fig. 8. SER versus average SNR per receive antenna for the STBC $\mathcal{C}_4$ with 16-QAM over i.i.d. and keyhole Nakagami-m fading channels. $n_R = 2$ and $m_T = m_R = m$ for keyhole channels.

For an arbitrary noninteger m, (20) and (22) can be evaluated in terms of the Gauss and Appell hypergeometric functions with the help of (43) and (48) in Appendix B, as shown in (23) and (24) at the bottom of the previous page. In (23) and (24), $\xi_{\mathrm{MPSK}} = g_{\mathrm{MPSK}}/(mn_TR)$ and $\xi_{\mathrm{MQAM}} = g_{\mathrm{MQAM}}/(mn_TR)$.

When m is a positive integer value, (20) and (22) can be expressed as closed forms in terms of finite sums of elementary functions by using the following results from [18, Appendix]:

$$\begin{aligned}\mathcal{I}_n(c,\psi) &\triangleq \frac{1}{\pi}\int_0^{\psi}\left(\frac{\sin^2\theta}{\sin^2\theta+c}\right)^n d\theta \\ &= \frac{\psi}{\pi}-\frac{\mu}{\pi}\Bigg[\left(\frac{\pi}{2}+\tan^{-1}\omega\right)\sum_{k=0}^{n-1}\binom{2k}{k}\frac{1}{[4(1+c)]^k} \\ &\quad +\sin(\tan^{-1}\omega) \\ &\quad \times\sum_{k=1}^{n-1}\sum_{i=1}^{k}\frac{T_{ik}\left[\cos(\tan^{-1}\omega)\right]^{2(k-i)+1}}{(1+c)^k}\Bigg], \\ &\quad n \text{ positive integer}, \quad -\pi\le\psi\le\pi \end{aligned} \tag{25}$$

where $\mu = \sqrt{c/(1+c)}\,\mathrm{sgn}(\psi)$, $\omega = -\mu\cot(\psi)$, and

$$T_{ik} = \frac{\binom{2k}{k}}{\binom{2k-2i}{k-i}4^i(2k-2i+1)}.$$

Applying (25) to (20) and (22), the average SERs of the STBC with M-PSK and M-QAM constellations over i.i.d. Nakagami-m fading channels for a positive integer m are given, respectively, by

$$P_{s,\mathrm{i.i.d.}}^{\mathrm{MPSK}}(E) = \mathcal{I}_{mn_Tn_R}\left(\frac{\xi_{\mathrm{MPSK}}E_s}{N_0}, \pi-\frac{\pi}{M}\right) \tag{26}$$

and

$$\begin{aligned}P_{s,\mathrm{i.i.d.}}^{\mathrm{MQAM}}(E) &= 4q\cdot\mathcal{I}_{mn_Tn_R}\left(\frac{\xi_{\mathrm{MQAM}}E_s}{N_0}, \frac{\pi}{2}\right) \\ &\quad -4q^2\cdot\mathcal{I}_{mn_Tn_R}\left(\frac{\xi_{\mathrm{MQAM}}E_s}{N_0}, \frac{\pi}{4}\right).\end{aligned} \tag{27}$$

B. Keyhole Nakagami-m Fading Channels

Taking the same steps as in Section IV-A, we can obtain the average SER of the STBC with M-PSK and M-QAM over keyhole Nakagami-m fading channels as integral expressions analogous to (20) and (22), respectively, only by replacing $\phi_{\gamma_{\mathrm{STBC}}}^{\mathrm{i.i.d.}}(\cdot)$ with $\phi_{\gamma_{\mathrm{STBC}}}^{\mathrm{keyhole}}(\cdot)$. The results are given by (28) and (29), shown at the bottom of the next page.

Unfortunately, the integrals in (28) and (29) do not have readily available closed-form solutions and, thus, one must evaluate these integrals numerically. Note that the hypergeometric functions ${}_2F_1$, F_1, and ${}_pF_q$ are provided as built-in functions in a common mathematical software package such as MATHEMATICA.

V. Simulations and Numerical Results

In this section, we provide the results of our analysis and compare them with simulation results in order to verify the analysis. For two, three, and four transmit antennas, we use the one-rate

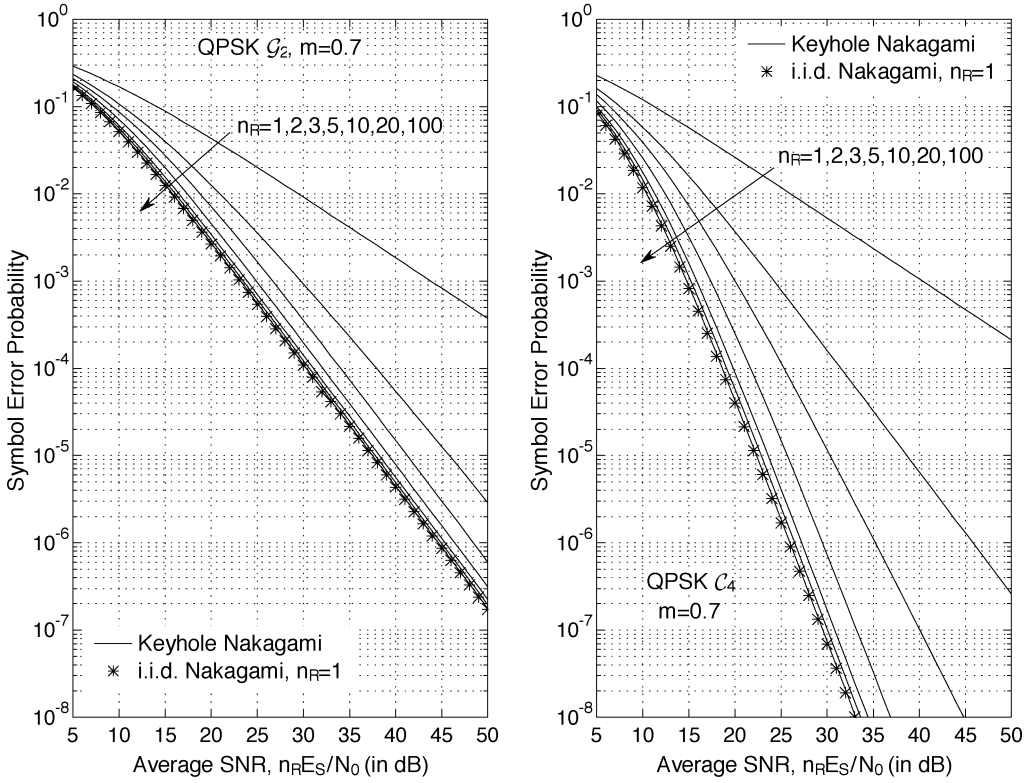

Fig. 9. SER versus average SNR $(n_R E_s/N_0)$ for the STBC $\mathcal{G}_2$ and $\mathcal{C}_4$ with QPSK over keyhole Nakagami-m fading channels when $n_R = 1, 2, 3, 5, 10, 20,$ and 100. For comparison, the SER for an i.i.d. Nakagami-m fading channel with one receive antenna is also plotted. $m_T = m_R = m = 0.7$.

STBC $\mathcal{G}_2$ (Alamouti code) and the following 3/4-rate codes, given in [9] and [15], respectively:

$$\mathcal{H}_3 = \begin{pmatrix} s_1 & s_2 & \frac{s_3}{\sqrt{2}} \\ -s_2^* & s_1^* & \frac{s_3}{\sqrt{2}} \\ \frac{s_3^*}{\sqrt{2}} & \frac{s_3^*}{\sqrt{2}} & \frac{-s_1-s_1^*+s_2-s_2^*}{2} \\ \frac{s_3^*}{\sqrt{2}} & -\frac{s_3^*}{\sqrt{2}} & \frac{s_1-s_1^*+s_2+s_2^*}{2} \end{pmatrix}$$

and

$$\mathcal{C}_4 = \begin{pmatrix} s_1 & s_2 & s_3 & 0 \\ -s_2^* & s_1^* & 0 & -s_3 \\ -s_3^* & 0 & s_1^* & s_2 \\ 0 & s_3^* & -s_2^* & s_1 \end{pmatrix}.$$

It should be noted that one can also design a simpler 3/4-rate STBC for three transmit antennas by dropping one column from $\mathcal{C}_4$, which is constructed from the unitary design [15].[4] In all examples, we set $m_T = m_R = m$ in keyhole Nakagami-m fading channels for the sake of a comparison with normal i.i.d. channels.

Figs. 3 and 4 show the SER versus average symbol SNR per receive antenna for the STBC $\mathcal{G}_2$ with 8-PSK and 16-QAM, respectively, over i.i.d. and keyhole Nakagmi-m fading channels for various values of m. These results are given for two receive antennas. The transmission rates of 8-PSK and 16-QAM $\mathcal{G}_2$ codes are 3 and 4 bits/s/Hz, respectively. Also, the SER for the STBC $\mathcal{H}_3$ and $\mathcal{C}_4$ with 8-PSK and 16-QAM are plotted in Figs. 5–8. Since $\mathcal{H}_3$ and $\mathcal{C}_4$ are 3/4-rate codes, the transmission rates for 8-PSK and 16-QAM are 2.25 and

[4] $\mathcal{C}_4$ has a simpler form than a 3/4-rate STBC $\mathcal{H}_4$ employing four transmit antennas given in [9] and can also be obtained by the unitary transformation of $\mathcal{H}_4$. The unitary transformations do not change the performance of the code.

$$P_{s,\text{keyhole}}^{\text{MPSK}}(E) = \frac{1}{\pi}\int_0^{\pi-\frac{\pi}{M}} {}_2F_0 \times \left(m_T n_T, m_R n_R;;-\frac{\frac{g_{\text{MPSK}}E_s}{N_0}}{m_T m_R n_T R\sin^2\theta}\right) d\theta. \tag{28}$$

$$P_{s,\text{keyhole}}^{\text{MQAM}}(E) = \frac{4q}{\pi}\int_0^{\frac{\pi}{2}} {}_2F_0\left(m_T n_T, m_R n_R;;-\frac{\frac{g_{\text{MQAM}}E_s}{N_0}}{m_T m_R n_T R\sin^2\theta}\right) d\theta - \frac{4q^2}{\pi}\int_0^{\frac{\pi}{4}} {}_2F_0 \times \left(m_T n_T, m_R n_R;;-\frac{\frac{g_{\text{MQAM}}E_s}{N_0}}{m_T m_R n_T R\sin^2\theta}\right) d\theta. \tag{29}$$

3 bits/s/Hz, respectively. From these figures, we see that the analysis agrees exactly with the simulation results and that the keyhole reduces the diversity improvement of the STBC, particularly in channels with a larger amount of fading (i.e., small values of the fading parameter m). This performance degradation is due to the fact that a keyhole channel has only a single degree of freedom and will fade twice as often as a normal i.i.d. channel. For $m = 1$ (Rayleigh case), the degradation due to the keyhole at the SER of 10^{-5} is approximately 15.5 dB for the 8-PSK $\mathcal{G}_2$, 16-QAM $\mathcal{H}_3$, and 16-QAM $\mathcal{C}_4$. The transmission rate in each case is 3 bits/s/Hz.

Fig. 9 shows the average SER versus average received SNR (i.e., $n_R E_s/N_0$) for quaternary PSK (QPSK) $\mathcal{G}_2$ and $\mathcal{C}_4$ over keyhole channels with $m = 0.7$ when $n_R = 1, 2, 3, 5, 10, 20$, and 100. For comparison, we also plot the average SER for the i.i.d. Nakagami-m fading channel with one receive antenna. For a fixed SNR $\rho \triangleq n_R E_s/N_0$ (irrespective of n_R), it follows that

$$\begin{aligned}\lim_{n_R\to\infty}\phi^{\text{keyhole}}_{\gamma_{\text{STBC}}}(s) &= \lim_{n_R\to\infty} {}_2F_0\left(mn_T, mn_R;;-\frac{s\rho}{m^2 n_T n_R R}\right)\\ &= {}_1F_0\left(mn_T;;-\frac{s\rho}{mn_T R}\right)\\ &= \left(1+\frac{s\rho}{mn_T R}\right)^{-mn_T}\\ &= \phi^{\text{i.i.d.}}_{\gamma_{\text{STBC}}}(s)\big|_{n_R=1} \end{aligned} \tag{30}$$

which shows that, as observed in Fig. 9, the average SER performance of the STBC over keyhole channels approaches that of the i.i.d. fading case with one receive antenna as the number of receive antennas increases. We can also see from (30) that the diversity order achieved by the STBC in the presence of the keyhole is limited to mn_T, as $n_R \to \infty$.

VI. Conclusion

We investigated the effect of keyholes, which make a MIMO channel exhibit uncorrelated spatial fading between antennas but a poor rank property, on the SER of STBCs. The fading between each pair of the transmit and receive antennas for keyhole channels was assumed to be characterized by a double Nakagami-m distribution. We derived the MGF of instantaneous symbol SNR after space–time block decoding and single finite-range integral expressions for the average SERs of the STBC with M-PSK and M-QAM constellations over keyhole Nakagami-m fading channels. In addition, we obtained an expression for the average SER for normal i.i.d. Nakagami-m fading in terms of the Gauss and Appell hypergeometric functions. These expressions are valid even for noninteger values of the Nakagami parameter m, unlike the closed-form expressions formerly known in the literatures of the analysis for diversity systems. Furthermore, we examined the AF to quantify the effect of keyholes on the severity of fading. It turns out that if the space–time block-coded MIMO link with n_T transmit and n_R receive antennas is degenerated by the keyhole effect, the severity of fading is increased by a factor of $(n_T + n_R + 1/m)$ and the achievable maximum diversity order is at most mn_T when $n_R \to \infty$.

Appendix A
PDF and MGF of a Product of Two Independent Gamma Variates

Let two independent random variables X and Y be gamma distributed, i.e., $X \sim \Upsilon(b_X, c_X)$ and $Y \sim \Upsilon(b_Y, c_Y)$, and $Z = X \cdot Y$ be a product of X and Y. Then the pdf of Z is given by

$$\begin{aligned} p_Z(z) &= \int_{-\infty}^{\infty} \frac{1}{|x|} p_X(x)\cdot p_Y\left(\frac{z}{x}\right)dx\\ &= \frac{2(b_X b_Y)^{-\frac{(c_X+c_Y)}{2}}}{\Gamma(c_X)\Gamma(c_Y)} z^{\frac{(c_X+c_Y)}{2}-1}\\ &\quad\cdot K_{c_Y-c_X}\left(2\sqrt{\frac{z}{b_X b_Y}}\right), \quad z \ge 0 \end{aligned} \tag{31}$$

where $K_\nu(\cdot)$ is the νth-order modified Bessel function of the second kind and its integral representation is given by [23, (8.432.6)]

$$\begin{aligned} K_\nu(u) &= \frac{1}{2}\left(\frac{u}{2}\right)^\nu \int_0^\infty t^{-(\nu+1)}\exp\left(-t-\frac{u^2}{4t}\right)dt,\\ &\quad |\arg u| < \frac{\pi}{2}, \quad \text{Re}\{u^2\} > 0. \end{aligned} \tag{32}$$

Using (32), we can find the MGF of Z as

$$\begin{aligned} \phi_Z(s) &\triangleq E[e^{-sZ}] = \int_0^\infty e^{-sz}\cdot p_Z(z)dz\\ &= \frac{(b_X b_Y)^{-c_Y}}{\Gamma(c_X)\Gamma(c_Y)} \int_0^\infty\int_0^\infty t^{c_X-c_Y-1}e^{-t}z^{c_Y-1}\\ &\quad\cdot\exp\left\{-\left(s+\frac{1}{b_X b_Y t}\right)z\right\}dtdz\\ &= \frac{1}{\Gamma(c_X)}\int_0^\infty t^{c_X-1}e^{-t}(1+b_X b_Y s t)^{-c_Y}dt\\ &= (b_X b_Y s)^{-c_X}\Psi\left(c_X, c_X-c_Y+1;\frac{1}{b_X b_Y s}\right) \end{aligned} \tag{33}$$

where $\Psi(a, b; x)$ is the confluent hypergeometric function [23, (9.211.4)]. From the identify ${}_2F_0(a, b;; -1/x) = x^a\Psi(a, a-b+1; x)$ [24, 6.6.(1)], we have

$$\phi_Z(s) = {}_2F_0(c_X, c_Y;; -b_X b_Y s) \tag{34}$$

where ${}_pF_q(a_1, a_2, \ldots, a_p; b_1, b_2, \ldots, b_q; x)$ is the generalized hypergeometric function [23, (9.14.1)], [24, 4.1.(1)].

The nth moment about the origin of Z is given by

$$\begin{aligned} E[Z^n] &= \int_0^\infty z^n p_Z(z)dz\\ &= \frac{(b_X b_Y)^n\Gamma(c_X+n)\Gamma(c_Y+n)}{\Gamma(c_X)\Gamma(c_Y)}\\ &= (b_X b_Y)^n (c_X)_n (c_Y)_n \end{aligned} \tag{35}$$

where $(a)_n = a(a+1)\cdots(a+n-1)$, $(a)_0 = 1$, $a \neq 0$, is the Pochhammer symbol.

APPENDIX B
INTEGRALS OF THE FORMS $\mathcal{J}_n(\omega,\psi) \triangleq (1/\pi)\int_0^{\pi-\psi}(\sin^2\theta/(\sin^2\theta+\omega))^n d\theta$, $0 \le \psi \le \pi/2$ AND $\mathcal{F}_n(\omega) \triangleq (1/\pi)\int_0^{\pi/4}(\sin^2\theta/(\sin^2\theta+\omega))^n d\theta$ FOR ARBITRARY REAL VALUES $n \ge 0$

In calculating the average SERs of the orthogonal STBC with M-PSK and M-QAM over i.i.d. Nakagami-m fading channels, we will need to evaluate

$$\mathcal{J}_n(\omega,\psi) = \frac{1}{\pi}\int_0^{\pi-\psi}\left(\frac{\sin^2\theta}{\sin^2\theta+\omega}\right)^n d\theta, \quad 0 \le \psi \le \frac{\pi}{2} \tag{36}$$

and

$$\mathcal{F}_n(\omega) = \frac{1}{\pi}\int_0^{\frac{\pi}{4}}\left(\frac{\sin^2\theta}{\sin^2\theta+\omega}\right)^n d\theta \tag{37}$$

which also appear in the analysis of single and multichannel reception of M-ary signals in Rayleigh- and Nakagami-m fading channels (e.g., see [17] and [19]). Although it is possible to express the closed-form solutions to these integrals with the results obtained from [18, (53)] and [19, (6)], those closed-form expressions are valid only for positive integer values of n. In this appendix, we obtain expressions for $\mathcal{J}_n(\omega,\psi)$ and $\mathcal{F}_n(\omega)$ in terms of the Gauss and Appell hypergeometric functions, which are available even if n is not restricted to positive integer values.

Dividing (36) into two integration parts as

$$\mathcal{J}_n(\omega,\psi) = \underbrace{\frac{1}{\pi}\int_0^{\frac{\pi}{2}}\left(\frac{\sin^2\theta}{\sin^2\theta+\omega}\right)^n d\theta}_{\triangleq I_1} + \underbrace{\frac{1}{\pi}\int_{\frac{\pi}{2}}^{\pi-\psi}\left(\frac{\sin^2\theta}{\sin^2\theta+\omega}\right)^n d\theta}_{\triangleq I_2}, \tag{38}$$

then, the first integration part of (38), I_1, can be rewritten as

$$I_1 = \frac{(1+\omega)^{-n}}{\pi}\int_0^{\frac{\pi}{2}}\left(\frac{\sin^2\theta}{1-\frac{\cos^2\theta}{(1+\omega)}}\right)^n d\theta. \tag{39}$$

Changing the variable $t = \cos^2\theta$ in (39), I_1 can be expressed as

$$\begin{aligned} I_1 &= \frac{(1+\omega)^{-n}}{2\pi}\int_0^1 t^{-\frac{1}{2}}(1-t)^{n-\frac{1}{2}}\left(1-\frac{t}{1+\omega}\right)^{-n} dt \\ &= \frac{(1+\omega)^{-n}}{2\sqrt{\pi}}\frac{\Gamma\left(n+\frac{1}{2}\right)}{\Gamma(n+1)}{}_2F_1\left(n,\frac{1}{2};n+1;\frac{1}{1+\omega}\right) \end{aligned} \tag{40}$$

where ${}_2F_1(a,b;c;x)$ is the Gauss hypergeometric function [23, (9.111)]. The second integration part of (38), I_2, can be rewritten as

$$\begin{aligned} I_2 &= \frac{1}{\pi}\int_{\psi}^{\frac{\pi}{2}}\left(\frac{\sin^2\theta}{\sin^2\theta+\omega}\right)^n d\theta \\ &= \frac{(1+\omega)^{-n}}{\pi}\int_{\psi}^{\frac{\pi}{2}}\left(\frac{\sin^2\theta}{1-\frac{\cos^2\theta}{(1+\omega)}}\right)^n d\theta. \end{aligned} \tag{41}$$

Changing the variable $t = \cos^2\theta/\cos^2\psi$ in (41), I_2 can be expressed as

$$\begin{aligned} I_2 &= \frac{(1+\omega)^{-n}\cos\psi}{2\pi} \\ &\quad\cdot\int_0^1 t^{-\frac{1}{2}}(1-t\cos^2\psi)^{n-\frac{1}{2}}\left(1-\frac{\cos^2\psi}{1+\omega}t\right)^{-n} dt \\ &= \frac{(1+\omega)^{-n}\cos\psi}{\pi} \\ &\quad\times F_1\left(\frac{1}{2},n,\frac{1}{2}-n;\frac{3}{2};\frac{\cos^2\psi}{1+\omega},\cos^2\psi\right) \end{aligned} \tag{42}$$

where $F_1(a,b,b';c;x,y)$ is the Appell hypergeometric function [24, 5.8.(5)]. From (38), (40), and (42), the integral $\mathcal{J}_n(\omega,\psi)$ with arbitrary $n \ge 0$ and $0 \le \psi \le \pi/2$ can be expressed as

$$\begin{aligned} \mathcal{J}_n(\omega,\psi) = (1+\omega)^{-n}\Bigg\{&\frac{1}{2\sqrt{\pi}}\frac{\Gamma\left(n+\frac{1}{2}\right)}{\Gamma(n+1)}{}_2F_1\left(n,\frac{1}{2};n+1;\frac{1}{1+\omega}\right) \\ &+\frac{\cos\psi}{\pi}F_1\left(\frac{1}{2},n,\frac{1}{2}-n;\frac{3}{2};\frac{\cos^2\omega}{1+\omega},\cos^2\omega\right)\Bigg\}. \end{aligned} \tag{43}$$

According to the reduction formula of the Appell hypergeometric function [24, 5.10.(10)]

$$F_1(a,b,b';c;x,1) = \frac{\Gamma(c)\Gamma(c-a-b')}{\Gamma(c-a)\Gamma(c-b')}{}_2F_1(a,b;c-b';x) \tag{44}$$

which can be obtained immediately from the Euler integral representation of F_1 [24, 5.8.(5)], for two extreme cases of $\psi = 0$ and $\pi/2$, (43) reduces to, respectively

$$\mathcal{J}_n(\omega,0) = \frac{(1+\omega)^{-n}}{\sqrt{\pi}}\frac{\Gamma\left(n+\frac{1}{2}\right)}{\Gamma(n+1)}\cdot{}_2F_1\left(n,\frac{1}{2};n+1;\frac{1}{1+\omega}\right) \tag{45}$$

and

$$\mathcal{J}_n\left(\omega,\frac{\pi}{2}\right) = \frac{(1+\omega)^{-n}}{2\sqrt{\pi}}\frac{\Gamma\left(n+\frac{1}{2}\right)}{\Gamma(n+1)}\cdot{}_2F_1\left(n,\frac{1}{2};n+1;\frac{1}{1+\omega}\right). \tag{46}$$

Note that we can easily show that (46) agrees with [18, (57)] by using the linear transformation of the Gauss hypergeometric function [23, (9.131.1)]

$${}_2F_1(a,b;c;x) = (1-x)^{c-a-b}{}_2F_1(c-a,c-b;c;x).$$

Next, $\mathcal{F}_n(\omega)$ can be rewritten as

$$\mathcal{F}_n(\omega) = \frac{(1+2\omega)^{-n}}{\pi}\int_0^{\frac{\pi}{4}}\left[\frac{\tan^2\theta}{1-\frac{1+\omega}{1+2\omega}(1-\tan^2\theta)}\right]^n d\theta. \tag{47}$$

Introducing a new variable $t = 1-\tan^2\theta$ in (47), we can evaluate the integral $\mathcal{F}_n(\omega)$ in terms of the Appell hypergeometric function as

$$\begin{aligned} \mathcal{F}_n(\omega) &= \frac{(1+2\omega)^{-n}}{4\pi} \\ &\quad\cdot\int_0^1(1-t)^{n-\frac{1}{2}}\left(1-\frac{t}{2}\right)^{-1}\left(1-\frac{1+\omega}{1+2\omega}t\right)^{-n} dt \\ &= \frac{(1+2\omega)^{-n}}{2\pi(2n+1)}F_1\left(1,n,1;n+\frac{3}{2};\frac{1+\omega}{1+2\omega},\frac{1}{2}\right). \end{aligned} \tag{48}$$

REFERENCES

[1] D. Chizhik, G. J. Foschini, and R. A. Valenzuela, "Capacities of multi-element transmit and receive antennas: Correlations and keyholes," *Electon. Lett.*, vol. 36, no. 13, pp. 1099–1100, 2000.

[2] D. Chizhik, G. J. Foschini, M. J. Gans, and R. A. Valenzuela, "Keyholes, correlations, and capacities of multielement transmit and receive antennas," *IEEE Trans. Wireless Commun.*, vol. 1, pp. 361–368, Apr. 2002.

[3] D. Gesbert, H. Bölcskei, D. A. Gore, and A. J. Paulraj, "Outdoor MIMO wireless channels: Models and performance prediction," *IEEE Trans. Commun.*, vol. 50, pp. 1926–1934, Dec. 2002.

[4] A. F. Molisch, "A generic model for MIMO wireless propagation channels," in *Proc. IEEE Int. Conf. Commun. (ICC) '02*, New York, Apr. 2002, pp. 277–282.

[5] V. Tarokh, N. Seshadri, and A. R. Calderbank, "Space–time codes for high data rate wireless communication: Performance criterion and code construction," *IEEE Trans. Inform. Theory*, vol. 44, pp. 744–765, Mar. 1998.

[6] J.-C. Guey, M. P. Fitz, M. R. Bell, and W.-Y. Kuo, "Signal design for transmitter diversity wireless communication systems," *IEEE Trans. Commun.*, vol. 47, pp. 527–537, Apr. 1999.

[7] S. M. Alamouti, "A simple transmit diversity technique for wireless communications," *IEEE J. Select. Areas Commun.*, vol. 16, pp. 1451–1458, Oct. 1998.

[8] V. Tarokh, H. Jafarkhani, and A. R. Calderbank, "Space–time block codes from orthogonal designs," *IEEE Trans. Inform. Theory*, vol. 45, pp. 1456–1467, July 1999.

[9] ——, "Space–time block coding for wireless communications: performance results," *IEEE J. Select. Areas Commun.*, vol. 17, pp. 451–460, Mar. 1999.

[10] X. Li, T. Luo, G. Yue, and C. Yin, "A squaring method to simplify the decoding of orthogonal space–time block codes," *IEEE Trans. Commun.*, vol. 49, pp. 1700–1703, Oct. 2001.

[11] S. Sandhu and A. Paulraj, "Space–time block codes: A capacity perspective," *IEEE Commun. Lett.*, vol. 4, pp. 384–386, Dec. 2000.

[12] G. Bauch and J. Hagenauer, "Smart versus dumb antennas—Capacities and FEC performance," *IEEE Commun. Lett.*, vol. 6, pp. 55–57, Feb. 2002.

[13] G. Bauch, J. Hagenauer, and N. Seshadri, "Turbo processing in transmit antenna diversity systems," *Ann. Telecommun.*, vol. 56, no. 7/8, pp. 455–471, 2001.

[14] G. Ganesan and P. Stoica, "Space–time block codes: A maximum SNR approach," *IEEE Trans. Inform. Theory*, vol. 47, pp. 1650–1656, May 2001.

[15] O. Tirkkonen and A. Hottinen, "Square-matrix embeddable space–time block codes for complex signal constellations," *IEEE Trans. Inform. Theory*, vol. 48, pp. 384–395, Feb. 2002.

[16] M. K. Simon and M.-S. Alouini, "A unified approach to the performance analysis of digital communication over generalized fading channels," *Proc. IEEE*, vol. 86, pp. 1860–1877, Sept. 1998.

[17] ——, *Digital Communication Over Fading Channels: A Unified Approach to Performance Analysis*. New York: Wiley, 2000.

[18] M.-S. Alouini and M. K. Simon, "Performance analysis of coherent equal gain combining over Nakagami-m fading channels," *IEEE Trans. Veh. Technol.*, vol. 50, pp. 1449–1463, Nov. 2001.

[19] A. Annamalai and C. Tellambura, "Error rates for Nakagami-m fading multichannel reception of binary and M-ary signals," *IEEE Trans. Commun.*, vol. 49, pp. 58–68, Jan. 2001.

[20] H. Shin and J. H. Lee, "Capacity of multiple-antenna fading channels: Spatial fading correlation, double scattering, and keyhole," *IEEE Trans. Inform. Theory*, vol. 49, pp. 2636–2647, Oct. 2003.

[21] U. Charash, "Reception through Nakagami fading multipath channels with random delays," *IEEE Trans. Commun.*, vol. COM-27, pp. 657–670, Apr. 1979.

[22] M. Evans, N. Hastings, and B. Peacock, *Statistical Distributions*, 3rd ed. New York: Wiley, 2000.

[23] I. S. Gradshteyn and I. M. Ryzhik, *Table of Integrals, Series, and Products*, 6th ed. San Diego, CA: Academic, 2000.

[24] A. Erdelyi, *Higher Transcendental Functions*. New York: McGraw-Hill, 1953, vol. 1.

Hyundong Shin (S'01) received the B.S. degree in electronics and radio engineering from Kyunghee University, Suwon, Korea, in 1999 and the M.S. degree in electrical engineering from Seoul National University, Seoul, Korea, in 2001. He is currently working toward the Ph.D. degree in electrical engineering at Seoul National University.

His current research interests include wireless communication and coding theory, turbo codes, space–time codes, and multiple-input–multiple-output (MIMO) systems.

Jae Hong Lee (M'86–SM'03) received the B.S. and M.S. degrees in electronics engineering from Seoul National University (SNU), Seoul, Korea, in 1976 and 1978, respectively, and the Ph.D. degree in electrical engineering from the University of Michigan, Ann Arbor, in 1986.

From 1978 to 1981, he was with the Department of Electronics Engineering, Republic of Korea Naval Academy, Jinhae, as an Instructor. In 1987, he joined the faculty of SNU. He was a Member of Technical Staff at the AT&T Bell Laboratories, Whippany, NJ, from 1991 to 1992. From 1992 to 1994, he served as the Chairman of the Department of Electronics Engineering, SNU. From 2001 to 2002, he served as the Associate Dean for Student Affairs, College of Engineering, SNU. Currently, he is with SNU as the Director of the Institute of New Media and Communications and as a Professor in the School of Electrical Engineering. His current research interests include communication and coding theory, code-division multiple access (CDMA), orthogonal frequency-division multiplexing (OFDM), and their application to wireless and satellite communications.

Dr. Lee is a Member of IEEK, KICS, KSBE, and Tau Beta Pi. He is a Vice President of the Institute of Electronics Engineers of Korea and of the Korea Society of Broadcasting Engineers. He is the Chairman of the Korea Chapter of the IEEE Vehicular Technology Society.